The Journal of Experimental Biology 212, 3605-3611
Published by The Company of Biologists 2009
doi:10.1242/jeb.033621

State-changes in the swimmeret system: a neural circuit that drives locomotion

N. Tschuluun, W. M. Hall and B. Mulloney*

Department of Neurobiology, Physiology and Behavior, and Center for Neuroscience, University of California Davis, One Shields Drive, Davis CA 95616-8519, USA

*Author for correspondence (bcmulloney@ucdavis.edu)

Accepted 20 August 2009

SUMMARY

The crayfish swimmeret system undergoes transitions between a silent state and an active state. In the silent state, no patterned firing occurs in swimmeret motor neurons. In the active state, bursts of spikes in power stroke motor neurons alternate periodically with bursts of spikes in return stroke motor neurons. In preparations of the isolated crayfish central nervous system (CNS), the temporal structures of motor patterns expressed in the active state are similar to those expressed by the intact animal. These transitions can occur spontaneously, in response to stimulation of command neurons, or in response to application of neuromodulators and transmitter analogues. We used single-electrode voltage clamp of power-stroke exciter and return-stroke exciter motor neurons to study changes in membrane currents during spontaneous transitions and during transitions caused by bath-application of carbachol or octopamine (OA). Spontaneous transitions from silence to activity were marked by the appearance of a standing inward current and periodic outward currents in both types of motor neurons. Bath-application of carbachol also led to the development of these currents and activation of the system. Using low Ca^{2+}–high Mg^{2+} saline to block synaptic transmission, we found that the carbachol-induced inward current included a direct response by the motor neuron and an indirect component. Spontaneous transitions from activity to silence were marked by disappearance of the standing inward current and the periodic outward currents. Bath-application of OA led promptly to the disappearance of both currents, and silenced the system. OA also acted directly on both types of motor neurons to cause a hyperpolarizing outward current that would contribute to silencing the system.

Key words: crayfish, acetylcholine, octopamine, excitation, inhibition, motor pattern.

INTRODUCTION

Effective behaviors require that activities of different parts of an animal's nervous system be integrated. This necessary coordination can be achieved by activation of particular neural circuits and silencing others that would interfere with a given behavior. To study the neural mechanisms that accomplish this coordination requires preparations that express behaviorally relevant activity and allow experimental access to the central nervous system (CNS). For three reasons, the crayfish swimmeret system is particularly suitable. (1) The isolated abdominal nerve cord will express the same motor output that drives normal swimmeret movements (Hughes and Wiersma, 1960; Ikeda and Wiersma, 1964). (2) A small set of identified axons that either excite or inhibit the expression of this motor output have been mapped in the abdominal cord (Wiersma and Ikeda, 1964; Atwood and Wiersma, 1967; Acevedo et al., 1994). (3) Responses of the system to stimulation of these axons are known in some detail (Acevedo et al., 1994).

Swimmerets are paired, jointed limbs located on segments of the abdomen. They are innervated by abdominal ganglia that are segmental components of the CNS. During forward swimming and certain other behaviors, swimmerets move rhythmically through cycles of power strokes (PS) and return strokes (RS) that propel the animal forward through the water. These movements are driven by alternating bursts of impulses in PS and RS motor neurons (Mulloney and Hall, 2000).

Both in the intact crayfish and in preparations of the isolated abdominal nerve cord, the swimmeret system can change state from inactive silence to active expression of the motor pattern. In the silent state, these neurons are predominantly silent. In the active state, bursts of spikes in PS motor neurons alternate with bursts of spikes in RS neurons innervating the musculature of the same swimmeret (Fig. 1). In the intact animal, transitions between the silent and active states are coordinated with other aspects of the animal's behavior. In isolated CNS preparations, these transitions sometimes occur spontaneously. Transitions can also be triggered by stimulating individual command neurons (Wiersma and Ikeda, 1964; Acevedo et al., 1994) and by pharmacological tools (Mulloney et al., 1987). Muscarinic agonists of acetylcholine elicit active expression of the motor pattern from silent preparations, and nicotinic agonists can then alter the period of the expressed pattern in a dose-dependent manner (Braun and Mulloney, 1993; Chrachri and Neil, 1993; Mulloney, 1997). Carbachol excites the swimmeret system, and has both nicotinic and muscarinic activity. However, octopamine (OA) silences active preparations (Fig. 1C), whether they are spontaneously active or have been pharmacologically excited (Mulloney et al., 1987).

To look more closely at mechanisms that activate or silence the system, we recorded membrane currents and measured input resistances of identified swimmeret motor neurons during transitions between active and silent states. We also recorded responses of motor neurons to carbachol and OA under conditions where these neurons were isolated from chemical synaptic input. Activation of the system was accompanied by the development of an inward current in both PS and RS motor neurons that served to depolarize these neurons. Using carbachol to excite the system led to two inward currents in these motor neurons, one elicited directly by carbachol and the other by indirect activation of a synaptic current. These inward currents were accompanied by decreases in the neurons' input resistances

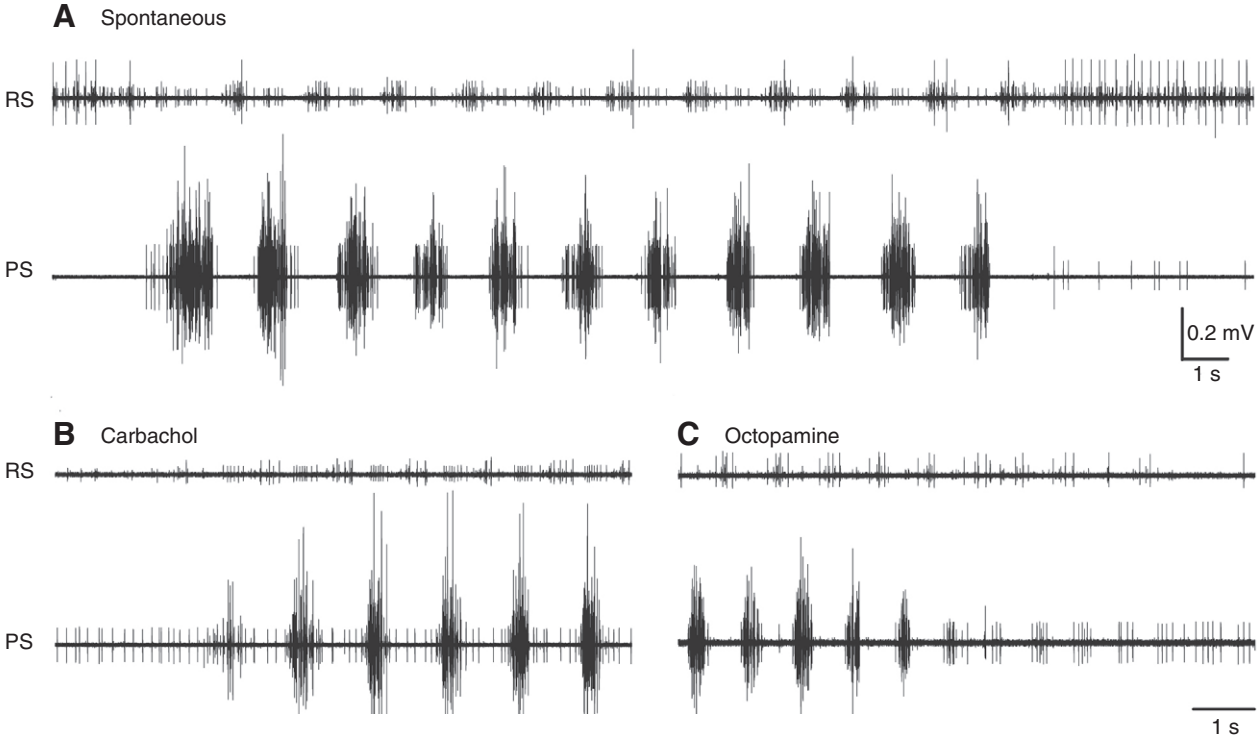

Fig. 1. State changes in the swimmeret system in three different isolated nerve-cord preparations. Power stroke (PS): extracellular recording from the power-stroke branch of the nerve innervating one swimmeret. Return stroke (RS): extracellular recording from the return-stroke branch of the same nerve innervating the same swimmeret. (A) Spontaneous transitions between the silent state and active expression of the normal swimmeret motor pattern in an isolated nerve-cord preparation perfused with normal saline. (B) A transition from silent to active expression of the swimmeret motor pattern caused by introduction of carbachol to the normal saline bathing the preparation. (C) A transition from active expression of the motor pattern to silence caused by introduction of octopamine (OA) to the bathing solution. In B and C, perfusion was switched from normal saline to carbachol or OA shortly before the beginning of these recordings.

and by the appearance of periodic inhibitory outward currents that shaped the bursts of action potentials in these neurons. Silencing the system was accompanied by disappearance of both the excitatory inward currents and the periodic inhibitory currents from motor neurons. OA elicited an inhibitory outward current directly in swimmeret motor neurons and also stopped the periodic inhibitory synaptic currents.

MATERIALS AND METHODS

Crayfish, *Pacifastacus leniusculus* Dana, were obtained from local commercial suppliers (Bob's Bait Shop, Isleton, CA, USA), and kept in aerated water tanks at temperatures 12–15°C. Normal saline consisted of (in $mmol\,l^{-1}$): 5.4 KCl, 2.6 $MgCl_2$, 13.5 $CaCl_2$, 195 NaCl, buffered with 10 $mmol\,l^{-1}$ Tris maleate at pH 7.4. Low Ca^{2+}–high Mg^{2+} saline was used to block synaptic transmission reversibly; it consisted of (in $mmol\,l^{-1}$): 5.4 KCl, 52 $MgCl_2$, 2.7 $CaCl_2$, 117 NaCl, buffered with 10 $mmol\,l^{-1}$ Tris maleate at pH 7.4.

Crayfish were anesthetized by chilling on ice and perfused with ice-cold crayfish saline. The anaesthetized animal was decapitated, and the chain of six abdominal ganglia (A1–A6) in the ventral nerve cord was removed. The nerve cord was pinned out dorsal-side up in a Sylgard-lined dish and desheathed with iridectomy scissors. This desheathing is important not only because it makes microelectrode work easier but also because it increases access of perfused drugs to the core of the CNS. These preparations were perfused with 2–3 ml of saline per minute. The perfusion line passed through an ice-filled bottle to cool the perfusion solution. In silent preparations, fictive locomotion was elicited by adding 1–6 $\mu mol\,l^{-1}$ carbachol to the perfusion solution [RBI, Natick, MA, USA; half-maximal dose (ED_{50}) 7.8 $\mu mol\,l^{-1}$ (Mulloney, 1997)]. To silence carbachol-elicited or spontaneous bursting, 50 $\mu mol\,l^{-1}$ OA was added to the perfusion [± octopamine hydrochloride, Sigma-Aldrich, St Louis, MO, USA; ED_{50} 50 $\mu mol\,l^{-1}$ (Mulloney et al., 1987)].

Electrophysiology

Each swimmeret is innervated by its own set of motor neurons whose cell bodies are located in clusters near the base of the nerve through which their axons project to their peripheral targets (Mulloney and Hall, 2000). There are four functional categories of these motor neurons that we can recognize in isolated preparations; about 35 power-stroke exciters (PSE) and two power-stroke inhibitors (PSI), about 35 return stroke exciters (RSE) and three return-stroke inhibitors (RSI) (Mulloney and Hall, 1990; Mulloney and Hall, 2000). In the present study, we focused on PSE and RSE neurons because they are relatively abundant. Only data from identified PSE and RSE neurons are included in this analysis.

Axons of swimmeret motor neurons project to their target muscles through the paired swimmeret nerves (N1) that project to each swimmeret from ganglia A2 through to A5 (Mulloney and Hall, 2000). Axons of PS and RS motor neurons then project into separate branches of each N1, so their firing can be recorded separately by pin electrodes in contact with these different branches (Fig. 1). These pin electrodes were connected to a switch box that allowed us to record or to stimulate with each electrode.

We recorded intracellularly from motor neurons in ganglia A3 and A4. Glass microelectrodes were used to penetrate their processes

in the ganglion's lateral neuropil, the locus of the local circuit that controls their firing (Mulloney et al., 2003). In active preparations, swimmeret motor neurons were initially identified by their oscillating membrane potentials, the phase of their bursts of spikes, and the time-locked spikes recorded by the microelectrode and a particular peripheral electrode. This identification was verified by antidromic action potentials triggered by stimulating the branch of N1 through the extracellular electrode. In most experiments, glass microelectrodes were filled with 1 mol l^{-1} potassium acetate + 0.1 mol l^{-1} KCl. Electrodes had resistances of about 30 MΩ. Signals from microelectrodes were amplified with an AxoClamp 2A amplifier (Molecular Devices Co., Union City, CA, USA). Signals from extracellular electrodes and the AxoClamp were digitized with a Digidata 1322A board controlled by Clampex software (Molecular Devices Co.). The sampling rate for digitizing was 10 kHz in order to capture extracellular spikes accurately.

In some experiments, neurons were also filled with a dextran-Texas Red marker for *post hoc* anatomical verification and classification. For this purpose, microelectrodes were filled with 1.0 mol l^{-1} KCl+10 mmol l^{-1} KPO_4+1% dextran-Texas Red (3 kDa; Invitrogen, Carlsbad, CA, USA). To fill individual neurons, the marker was injected electrophoretically using +1 nA, 250 ms current pulses at 2 Hz for at least 15 min. Once cells were filled, preparations were transferred into a Sylgard-lined dish and fixed overnight with 4% paraformaldehyde at 4°C. Preparations were then rinsed, dehydrated and cleared, and examined as whole-mounts with an Olympus Fluoview confocal microscope (Olympus America, Center Valley, PA, USA) (Mulloney and Hall, 2003).

Discontinuous current clamp (DCC) and single-electrode voltage clamp (dSEVC)

In both DCC and dSEVC modes, the settling time between current pulses was monitored continuously on a dedicated oscilloscope. To minimize electrode capacitance and so maximize the sampling frequency, the tips of microelectrodes were coated with Sylgard 186, only the tips were filled with electrode solution, and the level of saline above the ganglion was kept as low as possible. Normally, a sampling rate of 5 kHz was achieved. In dSEVC mode, the electrode potential was continuously monitored to ensure proper settling, and the command potential was adjusted manually using the holding-position potentiometer of the AxoClamp.

To measure input resistances, trains of –0.4 nA current pulses, 50 ms long were injected at different phases in the cycle of motor output using DCC. These pulses were triggered by bursts of spikes in PS axons using an episodic-stimulus protocol in Clampex. The changes in membrane potential caused by these stimuli were averaged and used to calculate input resistance. To permit comparisons of results from different neurons, each neuron's input resistances were normalized as a percentage of the maximum value recorded from that neuron. Differences between input resistances recorded at different phases were compared using one-way analysis of variances (ANOVAs) (Holm–Sidak method) in SigmaStat 3.5 (Systat Software, San Jose, CA, USA). Data were plotted as means±standard deviation (±s.d.) using SigmaPlot 10 (Systat Software).

Signal processing

To examine slow changes in membrane potentials and currents recorded continuously for many minutes, we filtered out the spikes and periodic oscillations that were superimposed on these slower changes. The upper limit of PS burst-frequency in the swimmeret system is about 4 Hz (Mulloney, 1997). Therefore, the raw data were low-pass filtered with a 4 Hz cut-off using a Gaussian algorithm in Clampfit (Molecular Devices Co.). The sampling frequency of the filtered recording was then reduced to 250 Hz while preserving maximum and minimum values. This reduction was done with Dataview (www.st-andrews.ac.uk/~wjh/dataview/). This sequence of steps removed the influence of fast events, like spikes, but retained the slower components that underlie periodic bursts of spikes in this system.

RESULTS

We set out to learn what occurs in swimmeret motor neurons when the system transitions between silent and active states (Fig. 1), and to investigate the actions of carbachol and OA on swimmeret motor neurons.

Transitions to activity are accompanied by an inward current

State transitions were detected by simultaneous recordings of activity in PS and RS branches of the swimmeret nerves (Fig. 1). We recorded membrane currents in swimmeret motor neurons during spontaneous transitions between silent and active states using dSEVC. In five preparations, spontaneous transitions occurred in normal saline (Fig. 2A). During each active state, an inward current developed in the clamped motor neuron that was periodically overridden by an inhibitory outward current (Mulloney, 2003). These inward currents ranged from –0.2 to –0.86 nA. When these same preparations were then bathed in carbachol saline, inward currents of similar amplitude continued to appear whenever bursts of spikes appeared on the PS recording (Fig. 2B).

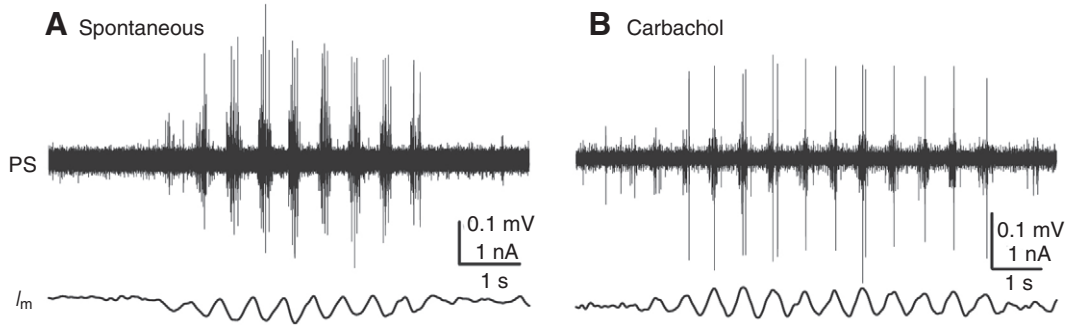

Fig. 2. Spontaneous transitions (A) and carbachol-induced transitions (B) from silence to active expression of the swimmeret motor pattern were accompanied by increases in inward membrane currents. (A) Membrane current (I_m) in a power-stroke exciter (PSE) motor neuron. Power stroke (PS): extracellular recording from the nerve that contained the axons of this PSE neuron. (B) I_m in a return-stroke exciter (RSE) motor neuron. PS: extracellular recording from the PS branch of the nerve innervating the same swimmeret as this RSE neuron. In both figures, the I_m traces were low-pass filtered (see Materials and methods).

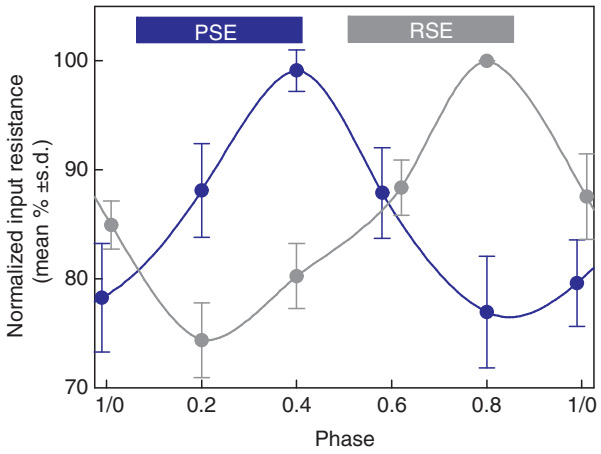

Fig. 3. Input resistances of power stroke and return stroke motor neurons change at different phases of the swimmeret motor pattern. Input resistances (means±s.d.) of power-stroke exciter (PSE) motor neurons (blue circles, *N*=16 neurons) and return-stroke exciter (RSE) motor neurons (gray circles, *N*=12 neurons) measured at different phases were normalized to the highest value recorded in each cell. The mean onset and duty cycle of the burst of spikes in PSE motor neurons is indicated by the blue bar, and of the burst in RS motor neurons by the gray bar. The points at 1/0 and 0.6 are slightly offset to avoid overlap.

Transitions to activity are accompanied by a decrease in input resistance

We measured the input resistances of PSE and RSE motor neurons in active preparations using DCC to inject current pulses at different phases in the motor pattern. To define the phase of the pulse within the cycle of activity, we measured the period of the cycle as the time from the start of the PS burst that preceded the current pulse to the start of the next PS burst, and the time delay from the start of the PS burst to the start of the current pulse. Phase was then the ratio of this delay to period, and could range between 0.0 and 1.0 (Fig. 3). Input resistance (MΩ) was calculated as the absolute value of the ratio of the change in membrane potential to the size of the current pulse (|mV/nA|).

The input resistance of most PSE neurons (18 out of 24) reached a maximum at phase 0.4 and its minimum at phase 0.8, during the RS burst (Fig. 3). At phases 0.4 and 0.8, these resistances were significantly different (P<0.001; one-way ANOVA). The input resistances of RSE motor neurons behaved similarly but with a shift of phase (Fig. 3). The input resistances of RSE neurons (10 out of 22) reached a maximum at phase 0.8 and a minimum at phase 0.2, during the PS part of the cycle. At phases 0.2 and 0.8, these resistances were significantly different (P<0.001; one-way ANOVA).

In preparations that were spontaneously active in normal saline, input resistances behaved in the same way as they did when activity was elicited by carbachol. Input resistances of PSE neurons (N=5) were highest during PS bursts and fell to a minimum during RS bursts. Input resistances of RSE neurons (N=5) reached their minimum during PS bursts and their maximum during RS bursts. Thus, both in spontaneously active preparations and in preparations excited by carbachol, swimmeret motor neurons fired bursts of spikes at the phase when their input resistances were high and fell silent as their input resistances fell due to inhibition by a periodic graded outward synaptic current (Mulloney, 2003).

Carbachol induced an inward current in swimmeret motor neurons

Perfusing silent preparations with carbachol saline elicited expression of the normal swimmeret motor pattern (Fig. 1B). We used dSEVC to record carbachol-elicited membrane currents from motor neurons in 19 initially silent preparations. As carbachol reached the preparations, bursts of spikes appeared on the PS recordings and a slow inward current developed on the current recording (Fig. 4A). The bursts of spikes in PS neurons and the inward current disappeared simultaneously when carbachol was washed out (Fig. 4B). In 10 PSE motor neurons, this inward current reached a plateau of –0.62±0.43 nA. In two RSE motor neurons, the inward current plateaued at –0.61±0.01 nA.

Carbachol-induced currents included both a synaptic and a direct component

Perfused drugs might act at any number of sites in the CNS, including directly on the motor neurons themselves. To look for such direct actions, we recorded membrane potentials or membrane currents in motor neurons when carbachol was introduced in the presence of low Ca^{2+}–high Mg^{2+} saline. Low Ca^{2+}–high Mg^{2+} saline effectively blocks chemical synaptic transmission in these preparations (Sherff and Mulloney, 1996; Tschuluun et al., 2001),

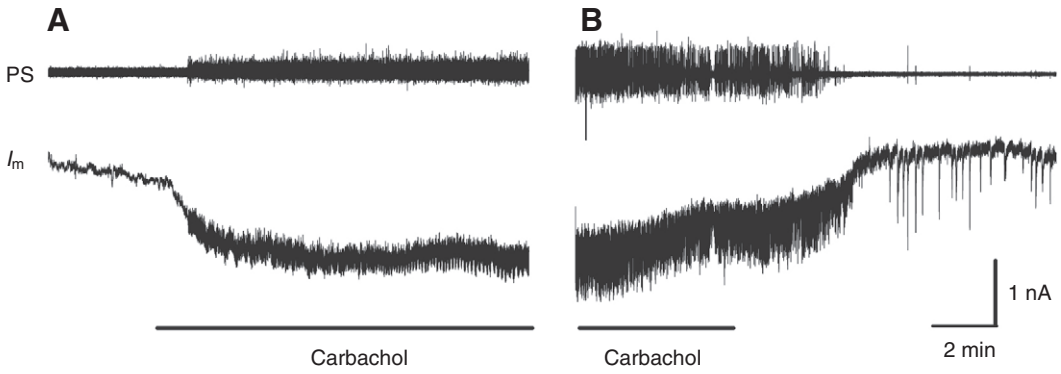

Fig. 4 Carbachol induced a steady inward current in swimmeret motor neurons. (A) Following the introduction of carbachol to the perfusion solution, power-stroke (PS) motor neurons began to fire bursts of spikes, and an inward current (I_m) appeared in this power-stroke exciter (PSE) motor neuron Once the PS motor neurons began to fire, the membrane current began to oscillate in response to periodic synaptic inhibition. (B) In a different PSE neuron, switching perfusion from carbachol saline to normal saline was followed by disappearance of the inward current and of the periodic oscillations that accompanied bursts of spikes in PS neurons. In both figures, the I_m traces were low-pass filtered (see Materials and methods).

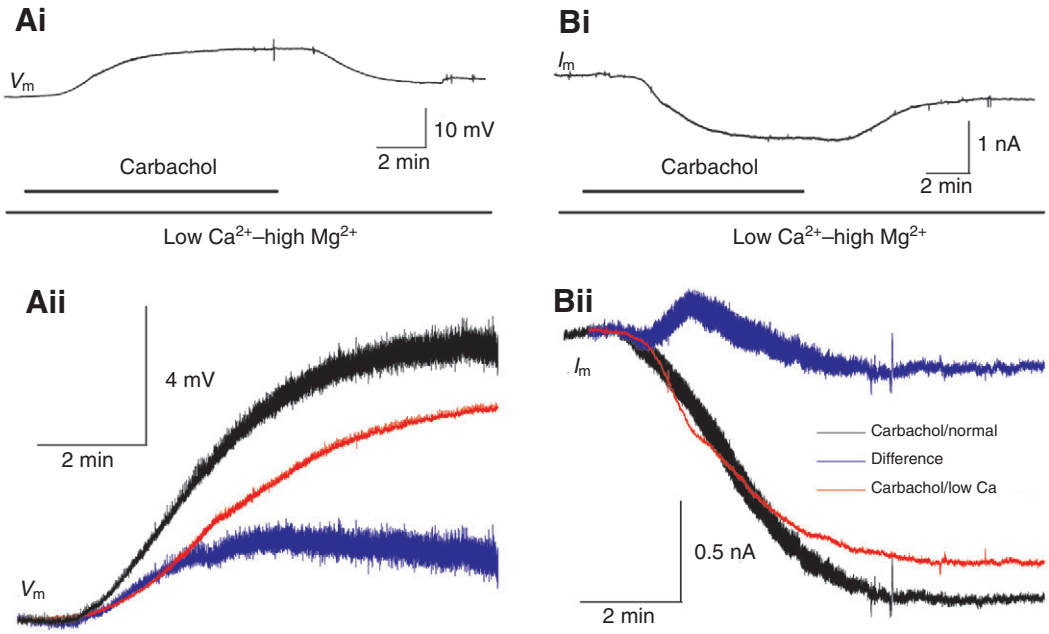

Fig. 5. The inward currents that appeared in swimmeret motor neurons perfused with carbachol result in part from a direct action of carbachol on the motor neuron. (Ai) Membrane potential (V_m) of a power-stroke exciter (PSE) neuron recorded in low Ca^{2+}–high Mg^{2+} saline during transient exposure to carbachol. (Aii) Superimposed recordings of V_m from the same neuron during two transient exposure to carbachol, one in normal saline (black) and the second in low Ca^{2+}–high Mg^{2+} saline (red). Subtraction of these two recordings reveals the change in potential caused by synaptic transmission during the active state (blue). (Bi) Membrane current (I_m) in another PSE neuron recorded in low Ca^{2+}–high Mg^{2+} saline during transient exposure to carbachol. (Bii) Superimposed recordings of I_m from this second PSE neuron during two transient exposures to carbachol, one in normal saline (black) and the second in low Ca^{2+}–high Mg^{2+} saline (red). The difference between these two recordings reveals the synaptic current from non-spiking premotor neurons (blue). In each panel, the V_m and I_m traces were low-pass filtered (see Materials and methods).

and should eliminate currents that appear in response to carbachol's actions on premotor interneurons. In 10 out of 16 PSEs and four out of four RSEs, carbachol addition under these conditions elicited a slow depolarization (Fig. 5Ai) or a slow inward current (Fig. 5Bi), depending on the mode of recording. The mean plateau of depolarization was 8.54±1.63 mV. The mean plateau of the inward current was –0.64±0.11 nA.

Carbachol in normal saline elicited larger depolarizations or larger inward currents than it did in low Ca^{2+}–high Mg^{2+} saline. When the same cells were exposed to the same concentrations of carbachol in normal saline and then in low Ca^{2+}–high Mg^{2+} saline, subtraction of the low Ca^{2+}–high Mg^{2+} recording from the normal saline recording yielded either a depolarizing potential (Fig. 5Aii) or an inward current (Fig. 5Bii). We attribute these to chemical synaptic input onto the motor neurons.

OA induced an outward current in swimmeret motor neurons

Because OA so effectively inhibits active expression of the swimmeret motor pattern (Mulloney et al., 1987), we looked for direct action of OA on swimmeret motor neurons. We used dSEVC to record changes in membrane currents when OA was applied in the presence of low Ca^{2+}–high Mg^{2+} saline. OA elicited an outward current from five out of six PSE and four out of six RSE motor neurons (Fig. 6B). The plateau values of these outward currents ranged between 0.2 nA and 0.5 nA, with a mean of 0.35 nA. From this evidence, at least part of the inhibitory effects of OA are achieved by eliciting a hyperpolarizing outward current directly in swimmeret motor neurons.

Both spontaneously active and carbachol-excited preparations were promptly silenced by introduction of OA to the perfusion solution (Fig. 1C). In four spontaneously active and eight carbachol-

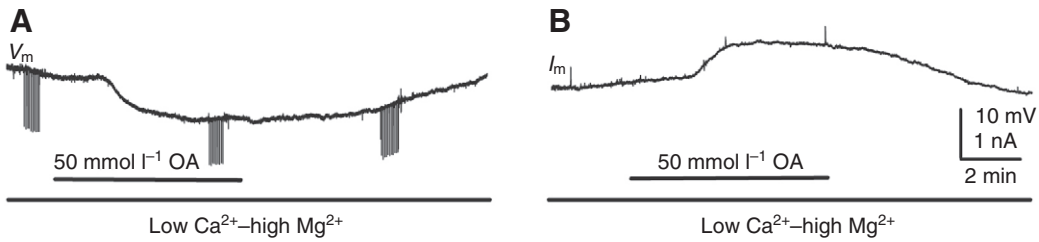

Fig. 6. Octopamine (OA) induced a steady outward current in swimmeret motor neurons. (A) Membrane potential (V_m) recorded from a power-stroke exciter (PSE) neuron during transient exposure to OA in the presence of low Ca^{2+}–high Mg^{2+} saline. The three bursts of deflections are responses to trains of brief current pulses that measured the neuron's input resistance. (B) Membrane current (I_m) of the same neuron during a second exposure to OA in low Ca^{2+}–high Mg^{2+} saline. Both recordings have been low-pass filtered (see Materials and methods).

excited preparations, we recorded changes in input resistances caused by OA. When OA was introduced, input resistances of six PSE motor neurons in carbachol and two in normal saline fell to the same level as the minimum reached during the normal cycle, 77±5% of the maximum resistance (Fig. 3). By contrast, input resistances of two RSE neurons in carbachol and two in normal saline fell only to 85±5% of maximum, a smaller change than that measured during the normal cycle, 74±3% (Fig. 3).

DISCUSSION

When the swimmeret system switches from an inactive to an active state, the motor neurons that control swimmeret movements depolarize and begin to fire (Fig. 1) because a new inward membrane-current develops (Fig. 2). The coordinated bursts of spikes that characterize their normal activity are then sculpted by periodic inhibitory synaptic currents common to all the motor neurons in each functional group: PSE, RSE, etc. (Mulloney, 2003). The presynaptic neurons causing these inhibitory currents are non-spiking local interneurons that form the kernel of the pattern-generating circuit that controls each swimmeret (Heitler and Pearson, 1980; Paul and Mulloney, 1985; Mulloney, 2003). These periodic currents are accompanied by significant oscillations in the motor neurons' input resistances. In different types of motor neurons, the maxima and minima of these oscillations occur at different phases. For PSE and RSI neurons, the maximum is near 0.4 and the minimum near 0.9 [see fig. 9 in Mulloney (Mulloney, 2003)]. For RSE and PSI neurons, the maximum is near 0.8 and the minimum near 0.2 [see figs 3 and 9 in Mulloney (Mulloney, 2003)].

Carbachol is a non-hydrolyzable agonist of acetylcholine at both muscarinic and nicotinic receptors and can excite the swimmeret system (Mulloney, 1997). Both PSE and RSE motor neurons responded directly to carbachol by depolarizing in response to an inward current (Fig. 5). Acetylcholine occurs as a neurotransmitter in many sensory afferent neurons in crustaceans and in all regions of the crustacean CNS including the abdominal ganglia (Hildebrand et al., 1974). It is the transmitter used by certain motor neurons in the crustacean stomatogastric system (Marder and Eisen, 1984). Other muscarinic analogues of acetylcholine (Braun and Mulloney, 1993; Chrachri and Neil, 1993), the neuropeptide proctolin (Acevedo et al., 1994) and Crustacean Cardioactive Peptide (CCAP), can also switch the swimmeret system from silence to active state (Mulloney et al., 1997). However, differences in the responses of PSE and RSE neurons to carbachol and CCAP suggest that their actions on the system are not identical. Both compounds depolarize PSE neurons directly but CCAP hyperpolarizes RSE neurons (Mulloney et al., 1997).

When carbachol elicits a transition to an active state, the inward currents it causes directly in motor neurons are paralleled by another inward current that disappears in low Ca^{2+}–high Mg^{2+} saline (Fig. 5). The current it elicited directly by bath-applied carbachol (Fig. 5) might flow through a ligand-gated receptor or through a channel modulated by a muscarinic pathway. Persistent sodium currents that are affected by neuromodulators occur in several other pattern-generating circuits (Harris-Warrick, 2002; Zhong et al., 2007). The current that disappears in low Ca^{2+}–high Mg^{2+} is probably the current that excites these neurons when the system switches spontaneously to the active state (Fig. 2). We postulate that this current is caused by transmitter released from an unidentified neuron, release that is blocked by low Ca^{2+}–high Mg^{2+}. We have seen no evidence that this excitatory current oscillates with the same period as the swimmeret motor pattern (Mulloney, 2003), so we think this postulated presynaptic neuron is not itself subjected to periodic synaptic input. Because this current does not oscillate periodically but can be abruptly terminated (Fig. 1C), we think that it might be due to graded transmitter-release from a presynaptic neuron that has two stable membrane potentials, one above the threshold for release and one below that threshold. Neurons that can switch between different stable membrane potentials have been described in other nervous systems (Opdyke and Calabrese, 1994; Svirskis and Hounsgaard, 1998; Viana di Prisco et al., 2000).

If the persistent current that disappears in low Ca^{2+}–high Mg^{2+} is either a Ca^{2+} current or a Ca^{2+}-gated current, an alternative interpretation of our results in Fig. 5 is possible. In other motor systems, both persistent low-voltage-activated Ca^{2+}-currents and Ca^{2+}-gated non-selective cation currents contribute to active states and plateau potentials (Harris-Warrick, 2002), and would be blocked by low Ca^{2+}–high Mg^{2+}saline. If swimmeret motor neurons express these currents, the disappearance of the inward current might not be due to blocking transmission but rather to reducing Ca^{2+} influx into the motor neurons themselves.

OA is a neurotransmitter that occurs in arthropod nervous systems (Roeder, 1999), and in neurons within crustacean abdominal ganglia (Schneider et al., 1993). Both PSE and RSE motor neurons are directly inhibited by OA (Fig. 6). This inhibition is accomplished by an outward current accompanied by a decrease in the neuron's input resistance. Glutamate and GABA also inhibit swimmeret motor neurons directly, by activating a chloride ion current (Sherff and Mulloney, 1996). For each of these three neurotransmitters, the decrease in input resistance that occurs when the transmitter in introduced is in the same range, about 25%. This suggests to us that although these transmitters probably bind to different receptors in the motor neurons, they act indirectly to gate the same chloride channel (Swensen and Marder, 2000). The inhibition of RSE neurons by CCAP, by contrast, is not accompanied by as large a decrease in input resistance and probably occurs by a different mechanism.

When OA inhibits the swimmeret system, the outward currents elicited in motor neurons are only part of the mechanism that silences the system. The periodic inhibitory currents that sculpt the bursts of spikes in these motor neurons also stop, so OA must also inhibit neurons in the premotor pattern-generating circuit.

ABBREVIATIONS

A1, A2, A3, A4, A5, A6	abdominal ganglia 1, 2, 3, 4, 5 and 6, respectively
CCAP	Crustacean Cardioactive Peptide
CNS	central nervous system
DCC	discontinuous current clamp
dSEVC	discontinuous single-electrode voltage clamp
I_m	membrane current
OA	octopamine
PS	power stroke
PSE	power-stroke exciter motor neuron
PSI	power-stroke inhibitor motor neuron
RS	return stroke
RSE	return-stroke exciter motor neuron
RSI	return-stroke inhibitor motor neuron
V_m	membrane potential

We thank Carmen Smarandache for thoughtful criticisms of the manuscript. Supported by NIH NINDS grant NS048149. Deposited in PMC for release after 12 months.

REFERENCES

Acevedo, L. D., Hall, W. M. and Mulloney, B. (1994). Proctolin and excitation of the crayfish swimmeret system. *J. Comp. Neurol.* **345**, 612-627.

Atwood, H. L. and Wiersma, C. A. G. (1967). Command interneurons in the crayfish central neurons system. *J. Exp. Biol.* **46**, 249-261.

Braun, G. and Mulloney, B. (1993). Cholinergic modulation of the swimmeret system in crayfish. *J. Neurophysiol.* **70**, 2391-2398.

Chrachri, A. and Neil, D. M. (1993). Interaction and synchronization between two abdominal motor systems in crayfish. *J. Neurophysiol.* **69**, 1373-1383.
Harris-Warrick, R. M. (2002). Voltage-sensitive ion channels in rhythmic motor systems. *Cur. Opin. Neurobiol.* **12**, 646-651.
Heitler, W. J. and Pearson, K. G. (1980). Non-spiking interactions and local interneurones in the central pattern generator of the crayfish swimmeret system. *Brain Res.* **187**, 206-211.
Hildebrand, J. G., Townsel, J. G. and Kravitz, E. A. (1974). Distribution of acetylcholine, choline, choline acetyltransferase and acetylcholine esterase in regions of single identified axons of the lobster nervous system. *J. Neurochem.* **23**, 951-963.
Hughes, G. M. and Wiersma, C. A. G. (1960). The co-ordination of swimmeret movements in the crayfish, *Procambarus clarkii*. *J. Exp. Biol.* **37**, 657-670.
Ikeda, K. and Wiersma, C. A. G. (1964). Autogenic rhythmicity in the abdominal ganglion of the crayfish: the control of swimmeret movements. *Comp. Biochem. Physiol.* **12**, 107-115.
Marder, E. and Eisen, J. S. (1984). Transmitter identification of pyloric neurons: electrically coupled neurons use different neurotransmitters. *J. Neurophysiol.* **51**, 1345-1361.
Mulloney, B. (1997). A test of the excitability-gradient hypothesis in the swimmeret system of crayfish. *J. Neurosci.* **17**, 1860-1868.
Mulloney, B. (2003). During fictive locomotion, graded synaptic currents drive bursts of impulses in swimmeret motor neurons. *J. Neurosci.* **23**, 5953-5962.
Mulloney, B. and Hall, W. M. (1990). GABAergic neurons in the crayfish nervous system: An immunocytochemical census of the segmental ganglia and stomatogastric system. *J. Comp. Neurol.* **291**, 383-394.
Mulloney, B. and Hall, W. M. (2000). Functional organization of crayfish abdominal ganglia: III. Swimmeret motor neurons. *J. Comp. Neurol.* **419**, 233-243.
Mulloney, B. and Hall, W. M. (2003). Local commissural interneurons integrate information from intersegmental coordinating interneurons. *J. Comp. Neurol.* **466**, 366-376.
Mulloney, B., Acevedo, L. D. and Bradbury, A. G. (1987). Modulation of the crayfish swimmeret rhythm by octopamine and the neuropeptide proctolin. *J. Neurophysiol.* **58**, 584-597.
Mulloney, B., Namba, H., Agricola, H. J. and Hall, W. M. (1997). Modulation of force during locomotion: differential action of crustacean cardioactive peptide on power-stroke and return-stroke motor neurons. *J. Neurosci.* **17**, 6872-6883.
Mulloney, B., Tschuluun, N. and Hall, W. M. (2003). Architectonics of crayfish ganglia. *Microscopy Res. and Tech.* **60**, 253-265.
Opdyke, C. A. and Calabrese, R. L. (1994). A persistent sodium current contributes to oscillatory activity in heart interneurons of the medicinal leech. *J. Comp. Physiol. A.* **175**, 781-789.
Paul, D. H. and Mulloney, B. (1985). Local interneurons in the swimmeret system of the crayfish. *J. Comp. Physiol. A.* **156**, 489-502.
Roeder, T. (1999). Octopamine in invertebrates. *Prog. Neurobiol.* **59**, 533-561.
Schneider, H., Trimmer, B. A., Rapus, J., Eckert, M., Valentine, D. E. and Kravitz, E. A. (1993). Mapping of octopamine-immunoreactive neurons in the central nervous system of the lobster. *J. Comp. Neurol.* **329**, 129-142.
Sherff, C. M. and Mulloney, B. (1996). Tests of the motor neuron model of the local pattern-generating circuits in the swimmeret system. *J. Neurosci.* **16**, 2839-2859.
Svirskis, G. and Hounsgaard, J. (1998). Transmitter regulation of plateau properties in turtle motoneurons. *J. Neurophysiol.* **79**, 45-50.
Swensen, A. M. and Marder, E. (2000). Multiple peptides converge to activate the same voltage-dependent current in a central pattern-generating circuit. *J. Neurosci.* **20**, 6752-6759.
Tschuluun, N., Hall, W. M. and Mulloney, B. (2001). Limb movements during locomotion: Tests of a model of an intersegmental coordinating circuit. *J. Neurosci.* **21**, 7859-7869.
Viana di Prisco, G., Pearlstein, E., Le Ray, D., Robitaille, R. and Dubuc, R. (2000). A cellular mechanism for the transformation of a sensory input into a motor command. *J. Neurosci.* **20**, 8169-8176.
Wiersma, C. A. G. and Ikeda, K. (1964). Interneurons commanding swimmeret movements in the crayfish, *Procambarus clarkii*. *Comp. Biochem. Physiol.* **12**, 509-525.
Zhong, G., Masino, M. A. and Harris-Warrick, R. M. (2007). Persistent sodium currents participate in fictive locomotion generation in neonatal mouse spinal cord. *J. Neurosci.* **27**, 4507-4518.